

39/2003

**Raport Badawczy**  
**Research Report**

**RB/29/2003**

**On the real-time  
emission control -  
case study application**

**P. Holnicki**

**Instytut Badań Systemowych**  
**Polska Akademia Nauk**

**Systems Research Institute**  
**Polish Academy of Sciences**



# **POLSKA AKADEMIA NAUK**

## **Instytut Badań Systemowych**

ul. Newelska 6

01-447 Warszawa

tel.: (+48) (22) 8373578

fax: (+48) (22) 8372772

Kierownik Pracowni zgłaszający pracę:  
Prof. dr hab. inż. Zbigniew Nahorski

Warszawa 2003

# On the real-time emission control – case study application

Piotr Holnicki  
Systems Research Institute  
Polish Academy of Sciences, Warsaw

**Keywords:** air pollution, mathematical modeling, emission control

**Abstract:** The paper presents formulation of the problem of real-time emission control in a predefined set of air pollution sources. The approach utilizes the optimal control technique for distributed parameter systems. The controlled object considered is a set of pointwise emission sources with a predefined location and emission characteristics. The problem is formulated as on-line minimization of an environmental cost function, by the respective modification of emission level in the controlled sources, according to the changing meteorological conditions (e.g. the wind direction and velocity). The environmental cost function depends on the current level of  $SO_x$  concentration and the sensitivity of the area to this type of air pollution. Dispersion of the atmospheric pollution is governed by a multi-layer dynamic model of  $SO_x$  transport, which is the main forecasting tool used in the optimization algorithm. The objective function includes the environmental damage related to air quality as well as the cost of the controlling action. The adjoint equation, related to the main transport equation of the forecasting model, is applied to calculate the gradient of the objective function in the main optimization procedure. The test computations have been performed for a set of the major power plants in the industrial region of Upper Silesia (Poland).

# 1 Air pollution forecasting model

The most common application of environmental models is forecasting of dispersion of pollutants. Air quality studies are also aimed at optimization, but numerous applications of optimization methods mainly occur in the design of monitoring networks. On the other hand, many important decisions in air pollution and environmental problems, which could be supported by the respective models, are directly made by decision makers. However, some optimization methods and environmental models give the possibility of implementation of air pollution control strategies.

For example, the long-term air pollution forecasting model was applied to evaluate the possible environmental consequences of the variant strategies of energy sector expansion in Poland [1]. The problem of the regional-scale strategy for emission abatement in a set of the major power plants was discussed in [10]. The solution of the last task is searched by the optimal selection of the desulfurization technologies for emission sources considered. From the viewpoint of the mathematical formulation, the above tasks are stated as static optimization problems.

Dynamic air pollution forecasting models can be used as a base for constructing the real-time emission control systems. In such a case, the optimal control problem is formulated as on-line minimization of an environmental cost function, by the respective modification of emission level in a set of the controlled sources, according to the changing meteorological conditions. The algorithms that solve such problems usually need certain procedure to evaluate the contribution of the controlled emission sources in the final environmental damage. This problem was discussed in [8].

It is assumed that the pollution transport process can be considered as distributed parameter system, governed by the transport equation. Implementation discussed in the sequel is sulfur-oriented, but the approach can be applied in a more general class of the forecasting models. The governing model generates short-term forecasts of air pollution related to a specified, complex emission field.

Computation of the transport of sulfur pollution is carried out by Lagrangian type, three-layer trajectory model [5, 7]. The mass balance for the pollutants is calculated for air parcels following the wind trajectories. The model takes into account two basic polluting

components: primary –  $SO_2$  and secondary –  $SO_4^{\pm}$ . Transport equations include chemical transformations  $SO_2 \Rightarrow SO_4^{\pm}$ , dry deposition and the scavenging by precipitation.

The main output constitutes the concentrations of  $SO_2$ , averaged over the discretization element and the vertical layer height. The governing equation, considered in one vertical layer, has the following, general form

$$\frac{\partial c}{\partial t} + \vec{v} \nabla c - K_h \Delta c + \gamma c = Q \quad \text{in} \quad \Omega \times (0, T), \quad (1)$$

along with the boundary conditions

$$c = c_b \quad \text{on} \quad S^- = \{\partial\Omega \times \langle 0, T \rangle \mid \vec{v} \cdot \vec{n} < 0\} \text{ - inflow of the domain,} \quad (1a)$$

$$K_h \frac{\partial c}{\partial \vec{n}} = 0 \quad \text{on} \quad S^+ = \{\partial\Omega \times \langle 0, T \rangle \mid \vec{v} \cdot \vec{n} \geq 0\} \text{ - outflow of the domain,} \quad (1b)$$

and the initial condition

$$c(0) = c_0 \quad \text{in} \quad \Omega. \quad (1c)$$

Here we denote

$\Omega$  – domain considered, with the boundary  $\partial\Omega = S^+ \cup S^-$ ,

$(0, T)$  – time interval of the forecast,

$c$  – pollution concentration,

$\vec{v}$  – wind velocity vector,

$\vec{n}$  – normal outward vector of the domain  $\Omega$ ,

$K_h$  – horizontal diffusion coefficient,

$\gamma$  – pollution reduction coefficient (due to deposition and chemical transformation),

$Q$  – total emission field.

The turbulent exchange of pollutants between layers usually is parameterized by introducing of the respective vertical diffusion coefficient [5, 6, 8].

The emission field on the right side of (1) can be expressed as follows:

$$Q(x, y, t) = q(x, y, t) + \sum_{i=1}^N \chi_i(x, y) q_i(t), \quad (2)$$

where

$q(x, y, t)$  – background (uncontrolled) emission field,

$q_i(x, y, t)$  – emission intensity of the controlled,  $i$ -th source,

$\chi_i(x, y)$  – characteristic function of the  $i$ -th source location.

Numerical algorithm is based on the discrete in time, finite element spatial approximation, combined with the method of characteristics [5, 6, 7]. The uniform space discretization step,  $h = \Delta x = \Delta y$  is applied in the computational algorithm. The mass balance for the pollutants is calculated for air parcels following the wind trajectories. Points along the trajectory are determined at discrete time points, based on the predefined interval  $\tau$ .

## 2 The optimal control problem

Basing on the forecasts of the pollution dispersion model, the real-time emission control problem for the system of sources located in the area can be formulated. The general idea of control consists in minimizing a predefined environmental cost function, according to changing meteorological conditions, by redistribution of energy production (emission intensity) within the set of the selected emission sources (controlled sources). Certain economic and technological constraints are also taken into account.

To formally state the optimal control problem, we below define the basic conditions. Assume that in a given domain  $\Omega$  there are  $N$  controlled emission sources described by certain spatial and temporal characteristics –  $\chi_i(x, y)$  and  $q_i(t)$ , respectively. There is also a set of uncontrolled emission sources  $Q$  that form the background pollution field.

**State equation.** We consider a concentration of the polluting factor  $c(x, y, t)$ , which satisfies the following transport equation

$$\frac{\partial c}{\partial t} + \vec{v} \nabla c - K_h \Delta c + \gamma c = Q + \sum_{i=1}^N \chi_i(x, y) F_i(u_i(t)) \quad \text{in } \Omega \times (0, T), \quad (3)$$

with the boundary conditions (1b) and the initial condition (1c). Function  $Q(x, y, t)$  represents an uncontrolled emission field (background emission). Emission characteristics of the controlled sources are represented by the product

$$q_i(x, y, t) = \sum_{i=1}^N \chi_i(x, y) F_i(u_i(t)) \quad \text{for } i = 1, \dots, N,$$

where  $\chi_i(x, y)$  describes the spatial location of the source, while  $F_i(u_i(t))$  is the temporal characteristics of emission intensity. Vector function  $\mathbf{u} = [u_1, \dots, u_N]^T$  denotes here the

control and represents production level (e.g. energy production of the power plant). Functions  $F_i$ , ( $i = 1, \dots, N$ ) relate energy production level of the respective plant, to the emission intensity, which is the right side of the state equation.

**Cost functional** to be minimized consists of two components: environmental cost function (air quality damage) and cost of the control. It is defined as follows

$$J(q) = \frac{\alpha_1}{2} \int_0^T \int_{\Omega} w [\max(0, c(\bar{u}) - c_{ad})]^2 d\Omega dt + \frac{\alpha_2}{2} \int_0^T \sum_{i=1}^N \beta_i (u_i(t) - u_i^*)^2 dt, \quad (4)$$

Here the coefficients  $\alpha_1$ ,  $\alpha_2$ ,  $\beta_i$ , ( $i = 1, \dots, N$ ) are given constants, where  $\alpha_1 \geq 0$ ,  $\alpha_2 \geq 0$ ,  $\beta_i > 0$ . The area sensitivity function satisfies the inequality  $0 \leq w(x, y) \leq 1$  and  $c_{ad}$  is a constant, admissible level of concentration. Functions  $u_i^*$ , ( $i = 1, \dots, N$ ) represent the nominal production level of the controlled source.

**Constraints** imposed on the production level of the controlled emission sources represent some technological and economic requirements, and are as follows

$$u_i \leq u_i(t) \leq \bar{u}_i(t) \quad \text{for } i = 1, \dots, N \quad (5a)$$

$$\sum_{i \in N_j} \delta_{ij} u_i(t) \geq d_j \quad \text{for } j = 1, \dots, M, \quad N_j \subset \{1, \dots, N\}. \quad (5b)$$

Inequalities (5a) are lower and upper technological limits on the real production level of the plant under consideration. Conditions (5b) represent constraints of total energy demand, which is imposed on the  $j$ -th subset of plants, with some coefficients  $\delta_{ij}$ .

We denote by  $K \subset H^1(0, T; R^N)$  the set of admissible controls of the form

$$K = \{\bar{u} \in H^1(0, T; R^N) : \bar{u} \text{ satisfies conditions (5)}\} \quad (6)$$

The state equation (3) has a unique solution  $c = c(\bar{u})$  determined for a given control  $\bar{u} \in L^2(0, T; R^N)$  and for fixed, constant parameters  $K_h, \gamma$ , where  $K_h > 0$ .

**Optimal control problem (P).** Find the element  $\bar{u}^o$  which minimizes the cost functional (4) over the set of admissible controls,

$$J(\bar{u}^o) = \inf_{\bar{u} \in K} J(\bar{u}),$$

where  $c(\vec{u}^\circ)$  satisfies the state equation (3).

We assume that there exists a constant  $\sigma > 0$  such that the following inequality holds

$$\langle DJ(\vec{u}) - DJ(\vec{v}), u - v \rangle > \sigma \|u - v\|_{H^1(0,T;R^N)}^2 \quad \forall u, v \in K, \quad (7)$$

where  $DJ(\vec{u})$  denotes the gradient of the functional (4). The last inequality is satisfied e.g. for  $F_i(u_i) = u_i$  and  $\alpha_i > 0, \beta_i > 0, \delta > 0$ . Condition (7) ensures the uniqueness (see [2, 4]) of the optimal solution in Problem (P).

**The optimality system for Problem (P).** It is known [2, 3, 4] that Problem (P) can be characterized as follows. Find  $(\vec{u}^\circ, c^\circ, p^\circ)$ , where  $\vec{u}^\circ = [u_1^\circ, \dots, u_N^\circ] \in K$ , such that

$$\frac{\partial c^\circ}{\partial t} + \vec{v} \cdot \nabla c^\circ - K \Delta c + \gamma c^\circ = Q + \sum_{i=1}^N \chi_i F_i(u_i^\circ) \quad \text{in } \Omega \times (0, T), \quad (8)$$

$$c^\circ = c_b^\circ \quad \text{on } S^- \quad (8a)$$

$$K \frac{\partial c^\circ}{\partial \vec{n}} = 0 \quad \text{on } S^+ \quad (8b)$$

$$c^\circ(0) = c_0^\circ \quad \text{in } \Omega. \quad (8c)$$

$$-\frac{\partial p^\circ}{\partial t} - \vec{v} \cdot \nabla p^\circ - K \Delta c + \gamma p^\circ = \alpha_1 w \max[0, c^\circ - c_d] \quad \text{in } \Omega \times (0, T), \quad (9)$$

$$p^\circ = 0 \quad \text{on } S^- \quad (9a)$$

$$K \frac{\partial p^\circ}{\partial \vec{n}} + \vec{v} \cdot \vec{n} p^\circ = 0 \quad \text{on } S^+ \quad (9b)$$

$$p^\circ(T) = 0 \quad \text{in } \Omega. \quad (9c)$$

$$\sum_{i=1}^N \{ \alpha_1 \int_0^T \int_\Omega \chi_i F_i'(u_i^\circ) p^\circ (v_i - u_i^\circ) d\Omega dt + \alpha_2 \int_0^T \beta_i (u_i^\circ - u_i^*) (v_i - u_i^\circ) dt \} \geq 0$$

$$\forall \vec{v} = [v_1, \dots, v_N] \in K. \quad (10)$$

Finite dimensional approximation of the problem (P) can be numerically solved by any gradient method. It follows from the optimality conditions [2] that the gradient of the cost functional (4) can be expressed as follows



$$D_i J(\bar{u}) = \alpha_1 \int_0^T \int_{\Omega} \chi_i F_i'(u_i^o) p^o d\Omega dt + \alpha_2 \int_0^T \beta_i (u_i^o - u_i^*) dt \quad (i = 1, \dots, N). \quad (11)$$

To calculate the gradient components according to (11), the following steps have to be performed in the consecutive iterations of the optimization procedure:

- solve the transport equation – problem (8),
- solve the adjoint equation (problem (9)) for the reversed time and the wind direction,
- substitute the adjoint variable  $p^*$  to (11) and calculate gradient components of environmental cost functional (4).

The next section presents the results of test computations performed for the real-data case study. The computational domain is a selected industrial region with the set of the major power plants, considered as the controlled emission sources.

### 3 The real-data case study

The general approach presented in Section 2 has been implemented and tested in a real data case. The test calculations have been performed for the set of the major power plants of the selected industrial region of Poland. To formally state the optimal control problem, which is to be solved, certain simplifications have been introduced to the general formulations discussed above.

We assume that the set of admissible controls  $U_{ad}$  is given by

$$U_{ad} = \{ \bar{u} \in L^2(0, T; R^N) \mid \bar{u}(t) \text{ satisfies (5a-b) for a. a. } t \in L^2(0, T; R^N) \}, \quad (12)$$

where condition (5b) has a form of a total energy demand constraint of the form

$$\sum_{i \in N} \delta_i u_i(t) \geq d. \quad (13)$$

Furthermore, we assume for simplicity that function that relates emission to production level,  $F_i$  in (3), is identity

$$F_i(u_i) = u_i, \quad i = 1, \dots, N. \quad (14)$$

The above relation means that we directly consider emission intensity of the source as the controlling function. The cost functional  $J(\bar{u})$  is defined by (4) for  $\bar{u} \in L^2(0, T; \mathbb{R}^N)$ ,  $\alpha_1 \geq 0$ ,  $\alpha_2 > 0$ , and  $\beta_i = \beta = 1$  for  $i = 1, \dots, N$ .

The test calculations have been performed for the selected region of Upper Silesia (Poland) and the set of 27 power plants, considered as the controlled emission sources. They represent the dominating power stations located within the region. Figure 1 presents the domain considered and the location of the controlled emission sources.

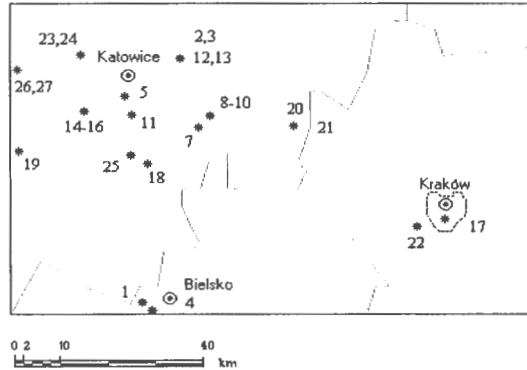


Figure 1: The computational domain and the emission sources

The computational domain constitutes a rectangle area  $110 \text{ km} \times 74 \text{ km}$ , which was discretized with the homogeneous grid with the space discretization step,  $h = 2 \text{ km}$ . This gives the discrete domain of the dimension  $55 \times 37$ . Surroundings of Kraków (indicated in Figure 1 with the dashed line) was defined as a region of high sensitivity, with the respective higher value of the area weight function,  $w(x, y)$ , in the cost functional (4),

$$w(x, y) = \begin{cases} 1 & \text{for } (x, y) \text{ in Kraków area,} \\ 0 & \text{for } (x, y) \text{ outside this area.} \end{cases} \quad (15)$$

Numerical implementation of the optimal control problem (P) discussed in Section 2 is based on the linearization method, by Pshenitchny [6, 11]. Computational results shown below represent real-time emission control for one 12-h time interval and a selected meteorological scenario. The nominal emissions of the controlled sources refer to the

winter season values, as presented in Table 1. Two cases of the optimal control problem, depending on the meteorological conditions, were considered

- **case A** – the West moderate wind, neutral atmospheric stability conditions,
- **case B** – the North-West moderate wind, neutral atmospheric stability conditions.

Grid coordinates and the main parameters of the controlled emission sources are presented in Table 1.

Table 1. List of the controlled  $SO_2$  emission sources

No.	Source	Source coordinates	Stack height [ m ]	Emission – winter [kg/h]	Emission – summer [kg/h]
1.	Bielsko-Biala	(14,2)	160	426.91	256.15
2.	Będzin A	(18,31)	95	94.89	63.25
3.	Będzin B	(18,31)	135	132.82	31.63
4.	Bielsko-Komorowice	(15,1)	250	426.91	189.74
5.	Chorzów	(12,27)	100	363.66	180.25
6.	Halemba	(8,25)	110	569.24	379.48
7.	Jaworzno I	(20,23)	152	284.61	158.12
8.	Jaworzno IIA	(21,24)	100	573.60	379.48
9.	Jaworzno IIB	(21,24)	120	664.08	426.91
10.	Jaworzno III	(21,24)	300	6324.60	4743.45
11.	Katowice	(13,25)	250	1106.81	790.58
12.	Łagisza A	(18,31)	160	948.69	695.71
13.	Łagisza B	(18,31)	200	1359.79	1011.94
14.	Łaziska I	(8,20)	200	1660.21	1185.86
15.	Łaziska II	(8,20)	160	758.95	505.97
16.	Łaziska III	(8,20)	100	727.95	505.97
17.	Łęg	(46,12)	260	1106.81	1.1
18.	Miechowice	(14,17)	68	161.28	117.01
19.	Rybnik	(1,20)	300	4711.83	3510.15
20.	Siersza A	(30,23)	150	1929.00	1423.04
21.	Siersza B	(30,23)	260	2055.49	1739.27
22.	Skawina	(43,11)	120	1992.25	1296.55
23.	Szombierki A	(9,31)	110	164.44	113.84
24.	Szombierki B	(9,31)	120	170.76	110.68
25.	Tychy	(13,19)	120	240.33	177.09
26.	Zabrze A	(2,29)	60	205.55	158.12
27.	Zabrze B	(2,29)	120	221.36	145.47

The FORTRAN 90 code of the optimization algorithm includes the forecasting model, the adjoint equation simulator and the optimization procedure, based on the Pschenitchny's method [11]. The computational experiments were performed on the UNIX platform server. Computing time required to find the optimal solution, in both scenarios considered is below 0.5 min. Some general results, concerning performance and the quality function reduction, are presented in Table 2.

Table 2. General results of 12-h simulation for two control tasks

Case	Number of iterations	Quality index – initial	Quality index – final	Reduction factor
A	3	10.7	7.1	30%
B	4	81.2	74.0	9%

The optimal control results related to modifications of the emission sources are shown in Table 3. They are expressed as factors related to the emission intensity of the selected sources (factor less than 1.0 means reduction of emission, factor greater than 1.0 – increase, respectively). Graphical presentation of the results for case A is shown in Figures 2 – 3. Figure 2 indicates the differences in the distribution of  $SO_2$  concentration for the reference emission field and for the emission control strategy implemented. The correlation between the adjoint variable distribution and the dominating controlled sources are seen in Figure 3. The area of high values of the adjoint variable shows locations of the sources, which significantly contribute in the overall environmental cost function. These sources have the emissions respectively reduced, as the result of the optimization algorithm. The quantitative results related this abatement scenario are shown in Table 3. The respective graphical results for the case B are shown in Figures 4 – 5, respectively.

The obtained results confirm the possibility of the effective utilization of the dispersion models and the discussed above technique in the real-time emission control. The accuracy and performance of the computer implementation of the model is satisfactory from the point of view of the possible future applications of this approach.

Table 3. Optimal emission control – modifications of the controlled sources

No.	Source	coordinates	height [ m ]	Emission kg/h]	control factor	
					case A	case B
1.	Bielsko-Biala	(14,2)	160	426.91	1.00	1.00
2.	Będzin A	(18,31)	95	94.89	1.00	1.00
3.	Będzin B	(18,31)	135	132.82	1.00	1.00
4.	Bielsko-Komorowice	(15,1)	250	426.91	1.00	1.00
5.	Chorzów	(12,27)	100	363.66	1.00	1.00
6.	Halemba	(8,25)	110	569.24	1.00	1.00
7.	Jaworzno I	(20,23)	152	284.61	1.00	1.00
8.	Jaworzno IIA	(21,24)	100	573.60	1.00	1.00
9.	Jaworzno IIB	(21,24)	120	664.08	1.00	0.80
10.	Jaworzno III	(21,24)	300	6324.60	1.04	0.80
11.	Katowice	(13,25)	250	1106.81	1.01	1.10
12.	Łagisza A	(18,31)	160	948.69	1.01	1.00
13.	Łagisza B	(18,31)	200	1359.79	1.01	0.90
14.	Łaziska I	(8,20)	200	1660.21	1.00	1.10
15.	Łaziska II	(8,20)	160	758.95	1.00	1.00
16.	Łaziska III	(8,20)	100	727.95	1.00	1.00
17.	Łęg	(46,12)	260	1106.81	1.00	1.10
18.	Miechowice	(14,17)	68	161.28	1.00	1.00
19.	Rybnik	(1,20)	300	4711.83	1.00	1.25
20.	Siersza A	(30,23)	150	1929.00	1.02	0.80
21.	Siersza B	(30,23)	260	2055.49	1.02	0.80
22.	Skawina	(43,11)	120	1992.25	0.82	1.10
23.	Szombierki A	(9,31)	110	164.44	1.00	1.00
24.	Szombierki B	(9,31)	120	170.76	1.00	1.00
25.	Tychy	(13,19)	120	240.33	1.00	1.00
26.	Zabrze A	(2,29)	60	205.55	1.00	1.00
27.	Zabrze B	(2,29)	120	221.36	1.00	1.00

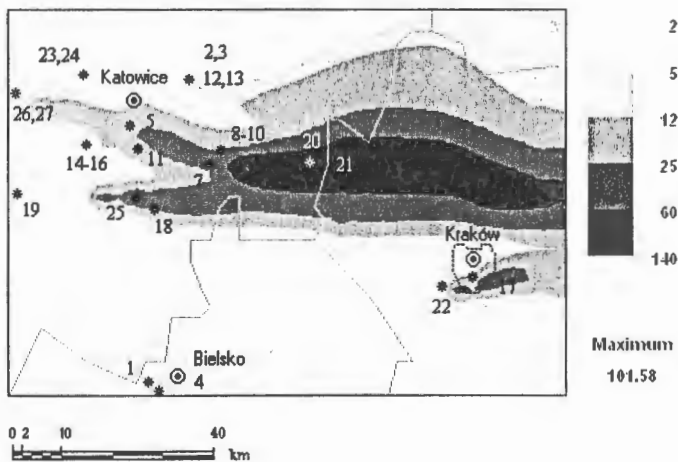
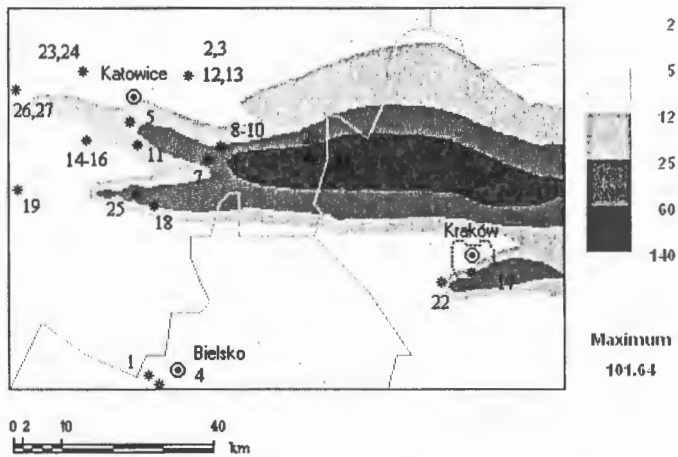


Figure 2: The initial (top) and the optimal (bottom)  $SO_2$  [ $\mu\text{g}/\text{m}^3$ ] concentration fields – case A

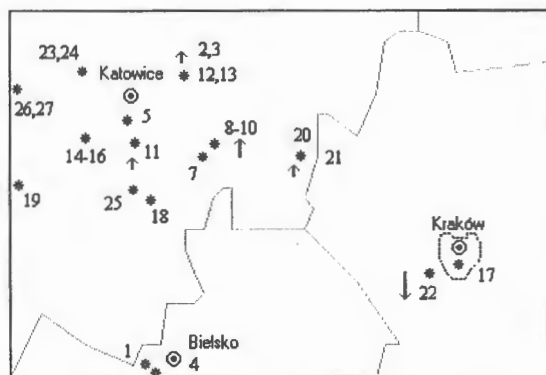
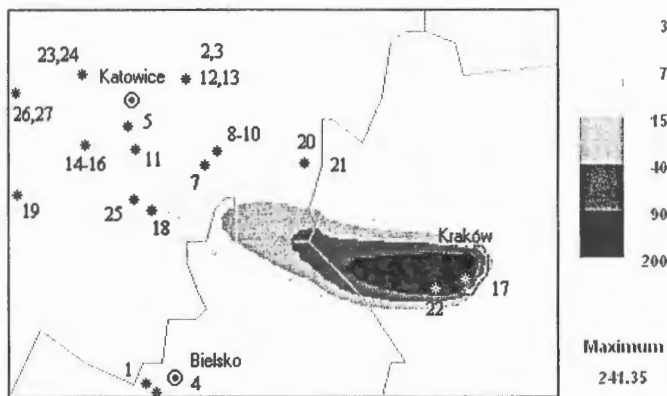


Figure 3: Distribution of the adjoint variable (top) and the changes of the controlled sources emissions (bottom) – case A

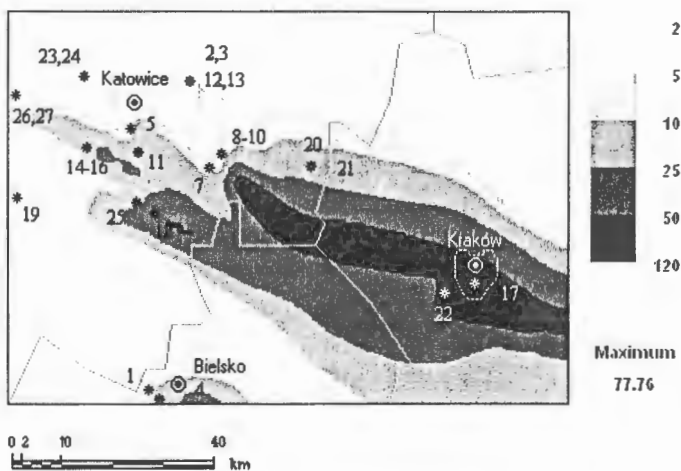
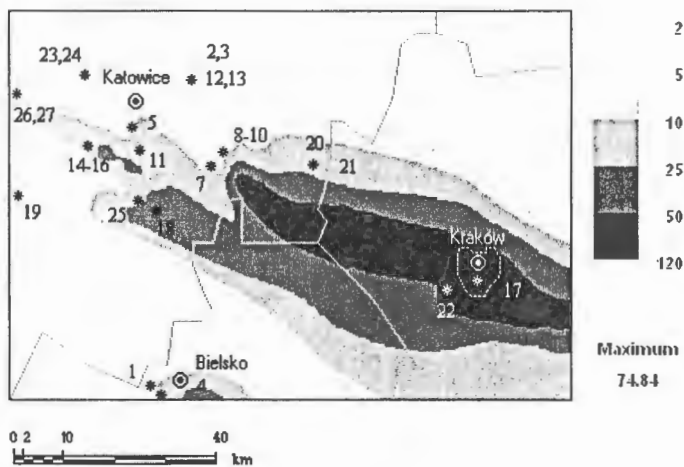


Figure 4: The initial (top) and the optimal (bottom)  $SO_2$  [ $\mu g/m^3$ ] concentration fields - case B



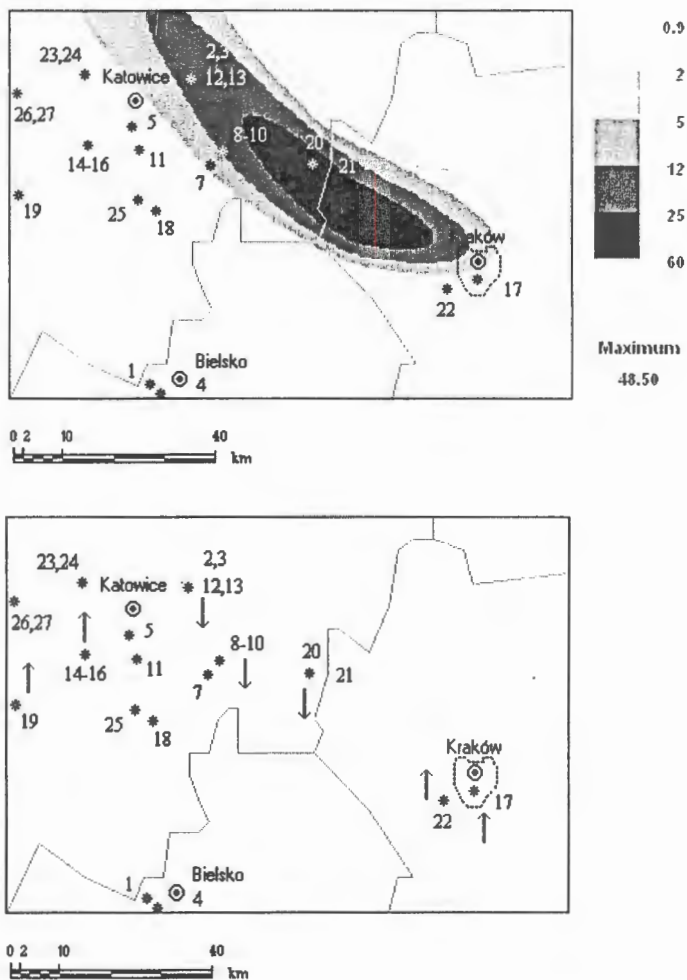


Figure 5: Distribution of the adjoint variable (top) and the changes of the controlled sources emissions (bottom) – case B

## References

- [1] Ciechanowicz W. et al. (1996) Energy and environment – problems of sustainable development, *Control and Cybernetics*, **25**, 1261–1271.
- [2] Lions J.L. *Optimal Control of Systems Governed by Partial Differential Equations*. Springer, New York 1971.
- [3] Lions J.L., Magenes E. *Problems aux limites non homogenes*. Dunod, Paris 1968.
- [4] Marchuk G.I. *Adjoint Equations and Analysis of Complex Systems*, Kluwer Academic Publishers, Dordrecht 1995.
- [5] Holnicki P., Kałuszko A. and A. Żochowski (1994) A microcomputer implementation of air quality forecasting system for urban scale, *Microcomputer Applications*, **13**, 76–84.
- [6] Holnicki P. and A. Żochowski *Wybrane metody matematyczne analizy jakości powietrza atmosferycznego*, PWN, Warszawa 1990.
- [7] Holnicki P. (1995) A shape preserving interpolation: applications to semi-Lagrangian advection, *Monthly Weather Review*, **123**, 862 - 870.
- [8] Holnicki P., Nahorski Z. and A. Żochowski *Modelowanie procesów środowiska naturalnego*, Wydawnictwa WSISiZ, Warszawa 2000.
- [9] Holnicki P., Żochowski A., Abert K. and K. Juda-Rezler (2001) Regional-scale air pollution dispersion model, *Environment Protection Engineering*, **33**, 133-145.
- [10] Holnicki P. and A. Kałuszko. A decision support system for air quality control based on soft computing methods. *Applied Decision Support with Soft Computing* (X. Yu, J. Kacprzyk – eds.), Springer, Berlin 2003, 290 – 3-7.
- [11] Pschenitchny B.N. *Metod linearizacji* (Russian), Nauka, Moskwa 1983.

## Appendix.

### Evaluation of environmental impact of emission sources

The main task in computational analysis of the real-time emission control is the finite-dimensional approximation of advection equation. Computational treatment of the advection-diffusion equations is difficult and needs carefully designed numerical algorithms. A class of effective and accurate numerical algorithms for solving the problem is based on semi-Lagrangian technique [6, 7]. Numerical scheme in this approach is usually constructed on regular mesh, follows wind-field characteristics backward in time and then employs polynomial interpolation of the departure profile at the upstream, departure point [7]. The main advantage of the approach, except numerical convenience of regular mesh discretization, is related to the fact that it admits relatively long time resolution step and is therefore computationally very efficient. However, the procedures applied for interpolation of the departure scalar field, and defined on a discretization mesh, often lead to nonphysical negative values or spurious oscillations, especially in regions of steep gradient. In order that the solution correctly reflects the initial profile suggested by the data, the approximation scheme must be positive definite (monotone if possible) and the numerical diffusion effect should be minimized. These negative effects can be especially dangerous in optimal control problems, because the uncorrect solution of the state equation is the right side of the adjoint equation. In case of improper numerical scheme this can generate significant errors in calculations of the gradient of the objective function. The above effects can significantly degrade the overall accuracy of the optimal control results.

A semi-Lagrangian transport algorithm investigated in the paper is based on the combination of the method of characteristics with a high degree polynomial interpolation of the departure profile, defined on a homogeneous grid. A 4-point interpolation stencil is used, with additional shape-preserving constraints imposed on the derivative estimates [7] at the internal interpolation points. The scheme considered is still computationally simple but it enables to obtain high overall accuracy of the solution due to the 5-th degree interpolation polynomial that can be applied for evaluation of the departure profile. On the

other hand, the scheme is relatively compact, which is an advantage for boundary conditions implementation. This is also an important point when local uniform grid refinement is used, since the required grid interfaces are then processed as domain boundaries.

The aim of the computational experiment was: i) to evaluate and compare the environmental impact of each source by the adjoint variable method, discussed in Section 2, ii) to examine accuracy of this technique, by comparing results to some reference data. The area sensitivity function  $w(x, y)$  introduced in relation (3), was defined according to (15) and indicates the Kraków region as the sensitive area (compare the dashed-line indicated area in Figures 2–5). Thus, the environmental impact of the sources under consideration was computed in the sense of deterioration of this domain.

To estimate accuracy of the results obtained by the adjoint variable algorithm, the reference influence of the emission sources was calculated. The relative contribution of a specific source has been directly obtained as the solution to problem (1), for the emission of this source reduced by 50%, with respect to the nominal emission intensity. This procedure was repeated in the sequel for all the sources, giving the respective set of the reference contributions of the controlled sources.

Test computations were performed for a selected, representative year (1996). The meteorological conditions are characterized by the respective sequence of 12-h sets of data. One-year interval was split down into four 3-month periods, and calculations were performed for 4 quarters, respectively. Selected numerical results are presented in Table 2. For a selected quarter, the neighbouring columns compare the relative impact of emission sources with the reference value. Both sets of results show the dominating impact of the source No. 22 (Skawina power plant) and the intermediate contribution of sources No. 10, 20, 21. On the other hand, there is a group of sources of minor or negligible influence, in the sense of the assumed criterion function.

Since the dimension of the adjoint variable depends on the form of equations (6), and has no a direct physical meaning – two columns in Table 2 can not be directly compared. Accuracy of computational method discussed was evaluated by correlation between computed and the reference data. The correlation coefficient of two sets of results is above  $R=0.97$  for all cases considered.

Table A1. Computed and the reference contribution of emission sources

No	Quarter 1		Quarter 2		Quarter 3		Quarter 4	
	Comp.	Refer.	Comp.	Refer.	Comp.	Refer.	Comp.	Refer.
1	1.22	0.13	0.20	0.35	0.43	0.50	0.53	0.11
2	0.08	0.16	0.05	0.26	0.07	0.12	0.19	0.23
3	0.11	0.20	0.03	0.14	0.04	0.08	0.28	0.21
4	2.07	0.01	0.43	0.10	0.40	0.05	1.62	0.02
5	0.30	0.22	0.24	0.63	0.22	0.44	0.21	0.28
6	0.54	0.26	0.48	1.06	0.37	0.33	0.26	0.32
7	0.54	0.48	0.43	0.49	0.22	0.77	0.75	0.24
8	0.81	1.00	1.04	0.31	0.61	0.80	0.83	1.10
9	1.16	0.44	1.36	0.48	1.13	0.80	1.07	0.88
10	31.65	9.59	10.71	6.44	33.82	13.20	23.26	4.44
11	2.39	0.78	1.14	1.50	4.01	1.26	1.57	0.50
12	0.63	0.89	0.55	1.94	1.32	1.13	1.79	1.17
13	3.17	1.33	0.77	2.42	2.64	0.81	2.33	1.59
14	1.79	0.17	1.21	2.06	0.89	0.25	1.15	0.31
15	0.81	0.11	1.09	0.87	0.47	0.14	0.47	0.16
16	0.77	0.24	0.71	1.27	0.43	0.40	0.46	0.31
17	7.67	0.08	9.46	1.08	12.08	0.62	0.05	0.02
18	0.20	0.05	0.23	0.28	0.11	0.05	0.14	0.06
19	3.87	0.50	6.04	3.50	1.39	1.05	2.21	1.03
20	34.41	6.41	12.70	16.23	20.28	13.72	22.08	5.96
21	40.44	4.14	18.80	15.08	21.00	11.43	25.09	4.43
22	204.49	59.95	77.31	67.59	156.53	72.17	230.75	62.49
23	0.08	0.05	0.12	0.24	0.12	0.12	0.10	0.06
24	0.09	0.04	0.10	0.23	0.09	0.09	0.11	0.06
25	0.29	0.05	0.33	0.44	0.18	0.18	0.18	0.08
26	0.15	0.04	0.12	0.25	0.11	0.11	0.06	0.06
27	0.16	0.04	0.12	0.24	0.08	0.08	0.06	0.07

Figure 6 presents the resulting maps of a long-term forecast (for the last quarter) of  $SO_2$  concentration and the related map of the adjoint variable distribution, calculated according to (9), for the reversed direction of time. Both maps show distributions of  $SO_2$  and the adjoint variable, averaged over the simulation period. The high values of the adjoint variable indicate the area of potentially high influence in sense of the index (4). This interpretation of adjoint variable is more directly seen in Figures 2 – 5, which show the respective maps for short-term forecast.

Environmental cost function (4), due to the transport equation (8), implicitly depends on the emission intensity of the controlled sources. Information about the quantitative contribution of emission sources in the total pollution field is necessary in some cases (for example in real-time emission control algorithms). A direct method of evaluation of this impact can utilize the consecutive reduction of emission level of the sources under question – the impact is represented by the related change of environmental cost index (4). In this approach, however, the main transport equation must be consecutively solved for all the sources considered. This means that in case of emission control, the most time-consuming step of the analysis has to be repeated many times.

Another approach, discussed in the sequel, utilizes optimal control techniques, namely the properties of the adjoint equation [2, 4], related to the state equation (1). Let  $\vec{q}(t) = [q_1(t), \dots, q_N(t)]$  denotes the vector function representing emissions of the controlled sources. Environmental cost index (4) can be considered as a function of  $\vec{q}$ , which means

$$J(q) = \frac{1}{T} \int_0^T \int_{\Omega} F(c(\vec{q})) d\Omega dt, \quad (16)$$

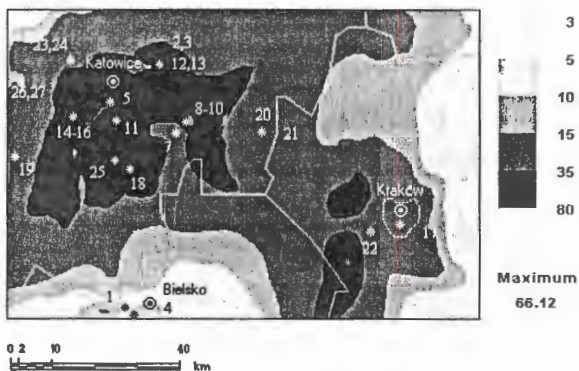
where subintegral function –  $F$ , according to (4), is expressed as

$$F(x, y, t) = w(x, y) [\max(0, c(x, y, t) - c_{ad}(x, y, t))]^2,$$

In order to evaluate sensitivity of the index (16) to the emission of the sources  $q_i(t)$ , ( $i = 1, \dots, N$ ), the gradient of this function must be computed. Assume a small change of emission level and denote by  $\epsilon \vec{s}$  the linear part of this change. Let  $\epsilon p$  be the respective change of concentration level, related to emission by (8). Thus, the respected disturbed

**SO<sub>2</sub> concentration forecast**

**Layer 1**

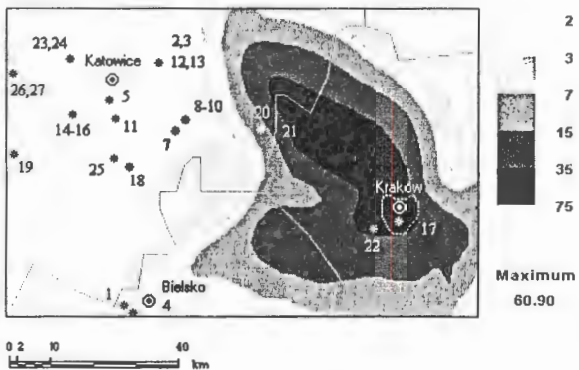


**Initial date 01/01/96**

**Time horizon 92 days**

**Distribution of the adjoint variable**

**Layer 3**



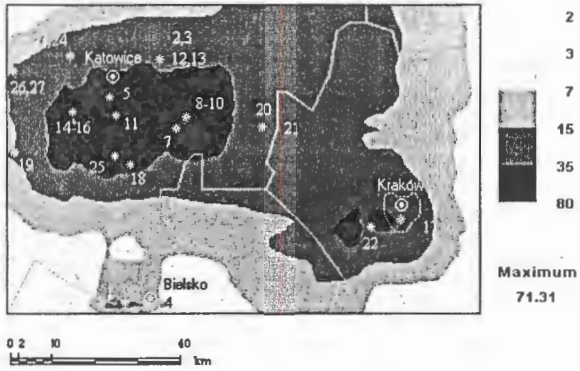
**Initial date 01/01/96**

**Time horizon 92 days**

Figure 6: The averaged (January-March)  $SO_2$  concentration forecast [ $\mu g/m^3$ ] (top), and the adjoint variable distribution (bottom)

**SO<sub>2</sub> concentration forecast**

**Layer 1**

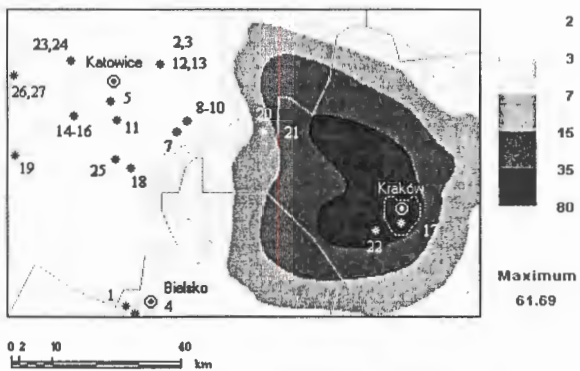


**Initial date 01/04/96**

**Time horizon 92 days**

**Distribution of the adjoint variable**

**Layer 3**



**Initial date 01/04/96**

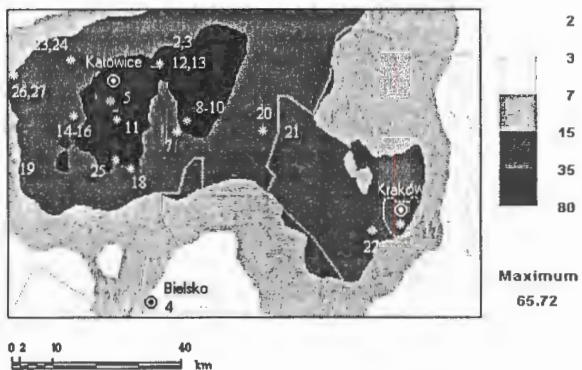
**Time horizon 92 days**

Figure 7: The averaged (April-June)  $SO_2$  concentration forecast [ $\mu g/m^3$ ] (top), and the adjoint variable distribution (bottom)



**SO2 concentration forecast**

**Layer 1**



**Distribution of the adjoint variable**

**Layer 3**

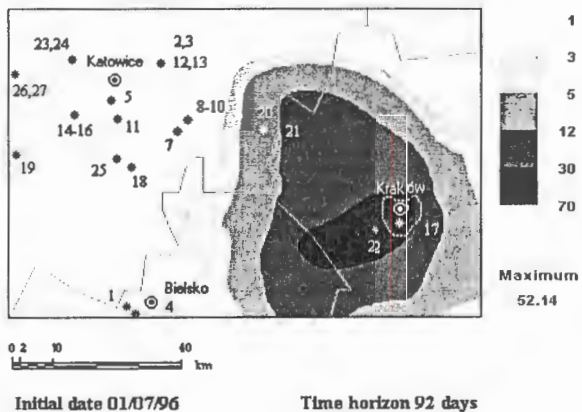
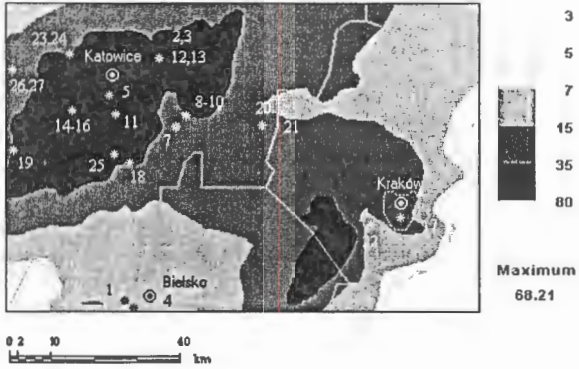


Figure 8: The averaged (July-September)  $SO_2$  concentration forecast [ $\mu g/m^3$ ] (top), and the adjoint variable distribution (bottom)

Season-averaged concentration forecast

Layer 1

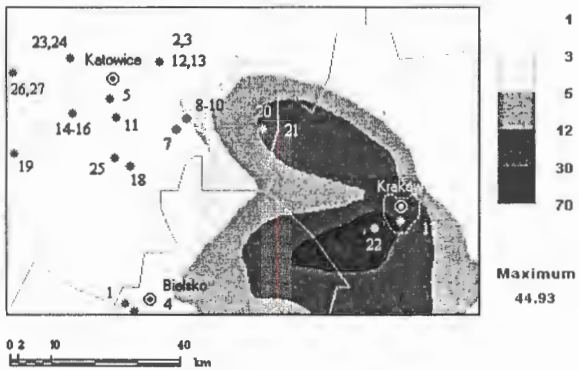


Initial date 01/10/96

Time horizon 92 days

Distribution of the adjoint variable

Layer 3



Initial date 01/10/96

Time horizon 92 days

Figure 9: The averaged (October-December) SO<sub>2</sub> concentration forecast [ $\mu\text{g}/\text{m}^3$ ] (top), and the adjoint variable distribution (bottom)

values are

$$\vec{q}_\epsilon = \vec{q} + \epsilon \vec{s} \quad \text{and} \quad c_\epsilon = c + \epsilon p.$$

Consequently, the linear part of the variation of the cost function (16) can be expressed in the form

$$\delta J = \frac{\epsilon}{T} \int_0^T \int_\Omega \frac{\partial F}{\partial c} p \, d\Omega \, dt, \quad (17)$$

where, according to (16), the derivative of subintegral function is as follows:

$$\frac{\partial F}{\partial c}(x, y, t) = 2w(x, y) \cdot \max[0, c(x, y, t) - c_{ad}(x, y, t)]. \quad (17a)$$

To calculate variation (17) – the value of function  $p$ , which is not explicitly available, must be known. Below the procedure based on the optimal control theory is presented, which allows to calculate this variation in one simulation run of the transport equation. It is known [2, 4] that the minimum of the index (4) is characterized as the solution of the state equation (1) and the solution  $p^*$ , of the following adjoint equation:

$$-\frac{\partial p^*}{\partial t} - \vec{u} \nabla p^* - K \Delta p^* + \gamma p^* = \frac{\partial F}{\partial c}(c) \quad \text{in} \quad \Omega \times (0, T), \quad (18)$$

along with the boundary conditions

$$p^* = 0 \quad \text{on} \quad S^-, \quad (18a)$$

$$K \frac{\partial p^*}{\partial \vec{n}} + (\vec{u} \cdot \vec{n}) p^* = 0 \quad \text{on} \quad S^+ \quad (18b)$$

and the final condition (for the end of the time interval)

$$p^*(T) = 0 \quad \text{in} \quad \Omega. \quad (18c)$$

It must be noted that equation (18) is solved for the negative time and the reversed direction of wind, while the right-hand side is the derivative of the subintegral function of environmental index (16). It can be shown [2] that, due to the specific form of the boundary conditions in (1) and (16), the increment of the cost function (17) can be expressed in the following form

$$\begin{aligned} \delta J &= \frac{\epsilon}{T} \int_0^T \int_\Omega p^* \sum_{i=1}^N \chi_i s_i \, d\Omega \, dt = \frac{\epsilon}{T} \sum_{i=1}^N \int_0^T \int_\Omega p^* \chi_i \, d\Omega \, s_i \, dt \\ &= \frac{\epsilon}{T} \sum_{i=1}^N \int_0^T G_i(t) s_i(t) \, dt, \end{aligned} \quad (19)$$

where we denote

$$G_i(t) = \int_{\Omega} p^*(x, y, t) \chi_i(x, y) d\Omega, \quad (i = 1, \dots, N).$$

The last relation makes it possible to calculate effectively the increment of the cost function, related to variation of the specific emission source. Our goal is to evaluate the contribution of each emission source in air quality deterioration. This contribution – in the sense of the measure (16) – can be calculated as the respective component of the following gradient function

$$\begin{aligned} \frac{\partial J}{\partial q_i} &= \lim_{\epsilon \rightarrow 0} \frac{\delta J}{\epsilon} = \frac{1}{T} \int_0^T G_i(t) s_i(t) dt \\ &= \frac{1}{T} \int_0^T \int_{\Omega} \chi_i(x, y) p^*(x, y, t) s_i(t) d\Omega dt, \quad (i = 1, \dots, N). \end{aligned} \quad (20)$$

Thus, to calculate the contribution of the emission sources one must successively perform the following steps

- solve the transport equation – problem (8),
- solve the adjoint equation (problem (18)) for the reversed time,
- substitute the adjoint variable  $p^*$  to (20) and calculate gradient components of environmental index (16).

To get the final solution, the transport and the adjoint equations must be solved only once. The method presented above has been applied for the real-data case study concerning the Upper Silesia region. Evaluation of the environmental impact of the major power plants has been performed by the adjoint variable algorithm.







